Clinics in Oncology

Research Article
Published: 26 Aug, 2022

Variations in Radiosensitivity of Breast Cancer and Normal Breast Cell Lines Using a 200 MeV Clinical Proton Beam

Peter du Plessis[1], Elsie Seane[2], Xanthene Miles[1], Shankari Nair[1], Jacobus Slabbert[1] and Charlot Vandevoorde[1]*

[1]*Department of Nuclear Medicine, Division of Radiation Biophysics, iThemba LABS (Laboratory for Accelerator Based Sciences), South Africa*

[2]*Department of Medical Imaging and Therapeutic Sciences, Cape Peninsula University of Technology, South Africa*

Abstract

Background: Worldwide, proton therapy is increasingly used as a radiation treatment alternative to photon therapy for breast cancer, primarily to decrease the risk for radiation-induced cardiovascular toxicity. However, uncertainties remain on the use of a constant Relative Biological Effectiveness (RBE) of 1.1 in clinical proton therapy. The beam at the position of the entrance plateau was used as the reference radiation in this study to signpost variation in RBE_{EP}.

Objectives: This *in vitro* study aimed to determine the radiosensitivity of both cancerous and non-cancerous breast cells to clinical proton irradiation. The variation in RBE at different depths along the proton Spread-Out Bragg Peak will be investigated.

Methods: Malignant (MCF-7) and non-Malignant (MCF-10A) breast cells were irradiated with doses ranging from 0.5 Gy to 4 Gy at 6 positions: the entrance plateau, 3 points on the Bragg peak (Proximal-, Middle- and Distal-SOBP), the 80% Dmax, and 40% Dmax. A Cytokinesis-Block Micronucleus (CBMN) assay was performed to determine cytogenetic damage using fluorescent microscopy.

Results: A gradual increase was observed in α parameters with depth for both cell lines. Variations in the RBE_{EP} between 0.99 to 1.99 for the cancerous cells and 0.92 to 1.60 for the non-cancerous breast cells, were observed. In fractionated proton therapy, the MCF-10A cells had a reduced repair in radiation-induced DNA damage between fractions compared to the cancerous MCF-7 cell line.

Conclusion: The RBE_{EP} results showed a clear increase in RBE_{EP} along the proton SOBP. This information could be used by the computational modeling community to further develop biologically motivated treatment planning for proton therapy. In addition, this study reveals a higher radiosensitivity for the non-cancerous breast cells.

Keywords: Breast cancer; Proton therapy; Cytokinesis-block micronucleus assay; MCF-7 cells; MCF-10A cells; Radiobiology; RBE; Hypofractionation

OPEN ACCESS

Correspondence:
Peter du Plessis, Department of Nuclear Medicine, Division of Radiation Biophysics, iThemba LABS (Laboratory for Accelerator Based Sciences), Cape Town, South Africa,
E-mail: pdp@tlabs.ac.za

Received Date: *28 Jul 2022*
Accepted Date: *19 Aug 2022*
Published Date: *26 Aug 2022*

Citation:
du Plessis P, Seane E, Miles X, Nair S, Slabbert J, Vandevoorde C. Variations in Radiosensitivity of Breast Cancer and Normal Breast Cell Lines Using a 200 MeV Clinical Proton Beam. Clin Oncol. 2022; 7: 1943.

ISSN: 2474-1663

Introduction

Breast cancer is at a steady increase among women with an age-adjusted incidence rate of 31.4 per 100,000 women and a lifetime risk of 1 in 29 [1]. The global estimate indicates that almost 62% of woman diagnosed in economically developing countries died of the disease. It remains the most common cancer in women of all races and, therefore, research for a more effective initial approach to diagnose and treat breast cancer patients in Africa remains a high priority [2]. However, in South Africa, around half of women diagnosed with breast cancer are estimated to survive 5 years [3]. Radiation Therapy (RT) plays an essential role in cancer treatment, which is based on the balance between cure and toxicity. Unfortunately, conventional photon-based RT will result in radiation exposure to healthy tissues and may be a key risk factor for developing subsequent contralateral breast cancer and cardiac side effects [4,5]. Particle therapy might provide a solution for the radiation-induced side effects. It was developed at scientific accelerator laboratories and remained a niche within radiation oncology during the last few decades. The clinical application of Proton Therapy (PT) is rapidly increasing over the last few years [6]. Globally, there are currently 109 proton-based treatment centers, of which 37 are located in the United States, based on the information from the particle therapy co-operative group updated in September 2020 [7]. Between 1954 and 2016, more than 149,000 patients have been treated with PT [8]. Protons deposit a low

dose in the entrance channel or plateau, followed by a steep increase and sharp dose fall-off towards the end of their range in the so-called 'Bragg peak'. A point in the spectrum beyond which no radiation dose is deposited [9]. In order to irradiate complete tumor regions of larger dimensions, a Spread Out Bragg Peak (SOBP) can be created [10].

With increasing clinical experience, advances in technology and dosimetry has allowed PT to slowly become an established alternative to conventional RT for the treatment of specific types of cancer, including breast cancer and childhood cancer [11,12]. One of the major concerns for breast cancer RT with photons is the potential increase in cardiac mortality related to radiation exposure to the heart [13-15]. Results from clinical trials have indicated that the use of PT for early breast cancer patients, either before or after mastectomy, is beneficial to reduce cardiac morbidity [16-18]. This is primarily due to the superior physical characteristics of protons compared to photons, resulting in a reduction of the radiation dose to the heart [19,20]. This may reduce the cardiac mortality in left breast cancer survivors receiving radical RT, thereby positively impacting breast cancer survival rates and reducing late side effects [17,21,22]. However, the dose sparing effects of PT might be outweighed by the usage of a fixed Relative Biological Effectiveness (RBE) for protons. RBE is defined as the ratio of the absorbed doses of two different radiation qualities to produce the same level of biological effect [23]. The RBE of protons is similar to MeV X-rays that are used in conventional RT and is set to be around 1.1 for therapeutic energy protons (up to 250 MeV) [24]. However, the RBE increases from 1.1 to 1.7 in the Bragg Peak where protons are slowing down towards the end of their range, resulting in an increase Linear Energy Transfer (LET) and higher biologic effectiveness. Indicative that sensitive, normal tissues should not be positioned immediately distal of the dose fall-off [23,25]. Thus, RBE variations should be considered as uncertainty bands when estimating normal tissue complications in the heart and lungs for breast cancer patients [26]. However, one of the current challenges is that the experimental basis for the variable RBE in PT lacks a significant number of representative tumor models and clinically relevant endpoints for dose-limiting organs at risk [27].

Various radiobiological endpoints can provide different insights into cellular radiosensitivity and could be used to determine RBE values relevant to normal tissue damage and carcinogenesis, such as chromosomal aberrations and DNA Double Strand Breaks (DSBs) repair [28]. The Cytokinesis-Block Micro Nucleus (CBMN) assay is one of the most common cytogenetic radiobiology assays used to evaluate cellular radiosensitivity [29]. The Micronuclei (MNi) represent a loss of genetic material that fail to attach to the mitotic spindle due to radiation-induced DNA damage. When a dose-response relationship is established for a specific radiation quality, the results can then be used to calculate the respective RBE for this type of radiation [30].

Thus, this study aimed to better understand the effects of protons on breast cancer cells by assessing genotoxicity and radiation-induced DNA damage at various positions along the proton depth dose profile. In addition, the aim was to determine whether there are variations in radiosensitivity and radiation-induced DNA damage between a cancerous and non-cancerous breast cell lines in response to 200 MeV proton radiations using the micronucleus assay.

Methods

Breast cell lines

Michigan Cancer Foundation-7 (MCF-7) cancerous breast cells were cultured using Dulbecco's Modified Eagle's medium F-12 (DMEM/F-12; Lonza, Walkersville, MD, USA) supplemented with 10% Fetal Bovine Serum (FBS), 1% antibiotics (penicillin and streptomycin; Lonza, Walkersville, MD, USA). Non-malignant MCF-10A breast epithelial cells were cultured using Dulbecco's Modified Eagle's Medium F-12 (DMEM F-12; Lonza, Walkersville, MD, USA) supplemented with 10% FBS (Gibco, Amarillo, Texas) and 1% penicillin/streptomycin. Moreover, the MCF-10A medium was supplemented with EGF (Epidermal Growth Factor; Sigma, Missouri, USA), hydrocortisone (0.5 mg/mL final concentration; Sigma, Missouri, USA) and insulin (10 µg/mL final concentration; Thermo Fisher Scientific, Waltham, Massachusetts, USA) the above-mentioned cell lines were cultured in an incubator at 37°C, 5% CO_2 air and humidified atmosphere.

Proton irradiation

Assessing the risk of secondary effects affecting the normal tissue (non-cancer cells) exposed at the beam entrance and fall-off was included for this investigation. In addition, MCF-10A cells were also irradiated at mid-SOBP positions to quantify if there were differences between the cancerous and non-cancerous cell line repair capacity. The approach was to use cancerous and non-cancerous epithelial cells that are similar in structure, location, and their functionality. While more biological endpoints should be investigated, and *in vivo* models should be used to improve our understanding of proton radiobiology, this study adds noteworthy information to the existing evidence base that there is an increase in RBE in the distal fall-off region relative to the proton beam entrance plateau. The cell lines were irradiated with a proton beam of an incoming energy of 200 MeV produced by the Separated Sector Cyclotron (SSC) at NRF-iThemba LABS, South Africa, in an in-house designed Perspex phantom with a positioning accuracy of 0.1 mm. The beam profile was checked by examining a depth-dose curve and checking the range, entrance dose, and the full width at half maximum of the Bragg peak were within prescribed limits according to NRF-iThemba LABS dosimetry standards [31]. The transverse profiles were checked for symmetry and flatness to ensure proper alignment of the beam. The scans were analyzed and checked for compliance with set limits. The SOBP of 5 cm was modulated using a rotating stepper-absorber (or a modulator wheel) and a monolayer of cells was irradiated in a 25 cm^2 cell culture flask at the different depths. Graded doses of 0.5, 1, 2, 3 and 4 Gy were given to the samples, while non-irradiated control samples were maintained, in the control room, receiving only ambient radiation exposure. Absolute dose measurements were performed by using the Markus chamber, a classic plane-parallel dosimetry chamber. The Markus chamber measurements were cross-calibrated against the reference chamber, and different output factors were measured for different depths as shown in Figure 1.

Cytokinesis block micronucleus (CBMN) assay

Immediately after radiation, 7.5 µL Cytochalasin B per 5.0 mL media (stock concentration 2.3 µL/mL) was added into each flask. Cultures were incubated for 48 h to inhibit cytoplasmic division and to enable MNi formation after anaphase division. Thereafter, the cells were trypsinated and harvested by washing with 5.0 mL hypotonic solution Potassium Chloride solution (KCl, pH 7.4). After centrifugation, the supernatant was removed, and the cell pellet was washed with 5.0 mL cold methanol/acetic acid/Ringer's solution (10:1:11) solution to fix the cells and maintain structural integrity. The samples were then diluted with methanol/acetic acid (10:1) solution and 3 slides per condition were prepared. Once air dried, slides were

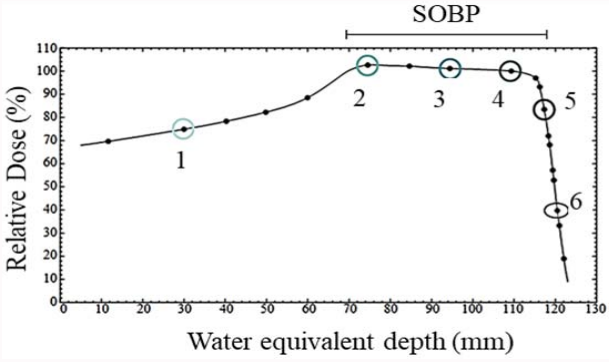

Figure 1: The six Water Equivalent Depths (WED) at which the two cell lines where irradiated within a proton beam (200 MeV incident energy). In sequential order are the entrance plateau, 3 points on the Bragg peak (Proximal-, Middle- and Distal-SOBP), the 80% Dmax and, 40% Dmax.

stained with Acridine Orange and scoring was performed as described in Vandersickel et al. [30]. A total of 500 Binucleated cells (BNCs) were manually scored per slide on a fluorescence microscope (Axio Imager. A1, Zeiss) by using the Fluorescein Isothiocyanate (FITC) filter. For each condition (cell line, dose point and position in the proton depth-dose curve), at least 1,500 BNCs were manually evaluated over three slides. The number of MNi induced by irradiation was obtained by subtracting the mean number of MNi in the non-irradiated controls from the mean MNi number scored in the irradiated samples. The CBMN assay enables more accurate scoring and the ability to sieve out the dividing cells from the non dividing ones, thereby reducing the incidence of false positives.

Bromodeoxyuridine (BrdU) and flow cytometric analysis

The BD Accuri™ C6 flow cytometer (BD Biosciences, California, USA) and FITC Bromodeoxyuridine (BrdU) flow kit to perform cell cycle analysis and determine the number of cells that are in S-phase. As radiosensitivity vary between cell cycle stages, it is important to take cell cycle kinetics into account, especially in the S-phase since these are known to be more radio resistant [32]. The protocol as described in the manufactures' instructions was followed. Cells were pulse labeled with BrdU by adding 250 µL of a 1 mM stock solution directly to 25 mL culture medium to give a final BrdU concentration of 10 µM. The cells were then incubated at 37°C/5% CO_2 for 15 min. One sample was then removed and immediately fixed, while in another sample the medium was replaced with fresh medium and the cells incubated for another 4 h at 37°C/5% CO_2. Cell samples were fixed in 70% ethanol for at least 30 min prior to antibody staining. Cells were centrifuged for 10 min at 805 g and the ethanol supernatant removed. The cell pellet was resuspended in 2.5 mL of 2 M HCl containing 0.2 mg/mL. Pepsin and incubated at room temperature for 20 min. Flow cytometric analysis was performed within 3 h after completion of staining. Both red and green fluorescence were collected as a linear signal. Cell doublets were eliminated by processing the red fluorescence into height, area and width (doublet discrimination mode). Data were collected in list mode and 10,000 events were recorded.

Data analysis

Statistical analysis and curve fitting were performed using Microsoft Office Excel 2013 (Microsoft Corporation, Washington, DC, USA) and GraphPad Prism Software Version 5.00 for Windows (GraphPad Software, San Diego, CA, USA). A program was developed on MATLAB (MATLAB for Deep Learning) platform to calculate the 95% confidence ellipse for the co-variance parameters α and β that describes the dose response curve for the average number of radiation-induced MN per 1000 BN cells. The program is based on the technique used by Slabbert et al. [33]. A two-sided $p<0.05$ was considered statistically significant.

The average number of MNi per dose point and cell line was plotted and dose-response curves were fitted by using a Linear-Quadratic (LQ) model, Equation 1.

Equation 1: The linear-quadratic equation

$$E = \alpha D + \beta D^2 + c$$

where E is the number of micronuclei observed in 1,000 binucleated cells, c the background frequency, α initial slope and β the bending component of each absorbed dose in Gy (D) response curve [34].

Thereafter, the RBE values were calculated using equation 2.

Equation 2: Equation to calculate the relative biological effectiveness for the same effect for different radiation modalities.

$$RBE = \frac{\text{Dose(Reference Radiation)}}{\text{Dose(Test Radiation)}} \text{Consequently},$$

$$RBE_{ep} = \frac{\text{Dose(Entrance Plateau)}}{\text{Dose(Test Positions)}}$$

The beam at the position of the entrance plateau was used as the reference radiation in this study, similar to previous studies performed at NRF-iThemba LABS, where the proton RBE was less than 3% for the entrance plateau [35]. Thus, the biological effectiveness will be associated to the entrance plateau of the proton beam, and be referred to as RBE_{ep}.

Results

The mean number of MNi/1000 BN cells was calculated for each cell line and dose response curves are presented in Figure 2 and Figure 3 based on non-linear regression analysis. The MNi were counted within BNCs to prevent confounding effects by suboptimal culture conditions [30].

From evaluating each position of the proton beam (Figure 4), the results indicated a difference in sensitivity between the two breast cell lines (p=0.01). Generally, the non-cancerous cells were more sensitive, in comparison to the cancerous breast cell line. As shown in Table 1, the β-values were negative after the initial fit. It is noted that a negative β-value is not acceptable, and selected data sets were refitted with a linear curve (β-value =0). Table 1 presents the coefficients of the fitted MN dose response curves based on the quadratic regression model for both cell lines after exposure to protons at different positions.

95% Confidence ellipse results

The ellipse region around a coordinate (the average MNi frequency) for both MCF-7 and MCF-10A cell lines defined by the mean estimate of the α-value plotted on the x-axis and the β-value on the y-axis is shown in Figure 5 for the entrance plateau region. The ellipse represents the inherent radiosensitivity of an individual (α-value) as well as the capacity to accumulate repairable damage (β-value). The two ellipses are distinctly separated from each other, which is indicative of an exclusive dose response relationship at the entrance plateau in the proton beam (used as reference radiation quality in this study). Suggesting that, there is a significant difference (p= <0.001) in radiosensitivity between the MCF-7 and MCF-10A cell

Table 1: Alpha and beta values calculated using the second order polynomial theorem. A (Background =a); B (Bending component =α); C (Initial slope =β). Both cell lines were fitted according to Polynomial: Second order ($Y=A+ B*X+ C*X^2$) best-fit values.

	PLAT	PROX SOBP	MID SOBP	DIS SOBP	80% DMAX	40% DMAX
MCF-10A						
A	26.67	26.67	26.67	26.67	26.67	26.67
B	113.1	140.7	67.96	157.2	192.6	181.1
C	7.25	0	20.91	0	0	0.18
MCF-7						
A	13.33	13.33	13.33	13.33	13.33	13.33
B	85.36	70.28	130.7	130.8	156.5	117.3
C	0	7.84	0	6.73	1.75	5.93

Table 2: Iso-effective doses calculated for both MCF-10A and MVF-7 cells at different levels of biological effects.

Normalised MNI	PLAT	PROX SOBP	MID SOBP	DIS SOBP	80% DMAX	40% DMAX
	DOSE (Gy) FOR MCF-10A					
100	0.65	0.55	0.85	0.47	0.5	0.41
200	1.44	1.3	1.68	1.11	1.18	0.96
300	2.16	2.05	2.34	1.75	1.87	1.51
400	2.82	2.8	2.9	2.39	2.55	2.06
500	3.44	3.55	3.4	3.03	3.23	2.61
	DOSE (Gy) FOR MCF-7					
100	1.06	1.1	0.67	0.64	0.55	0.71
200	2.26	2.14	1.45	1.34	1.18	1.48
300	3.55	3.04	2.23	1.99	1.8	2.2
400	4.9	3.84	3.03	2.61	2.41	2.88
500	6.33	4.58	3.84	3.2	3.01	3.52

lines.

Figure 6 represents the 95% confidence ellipse for MCF-7 and MCF-10A cells at the different positions along the proton SOBP. For both cell lines, there is an increasing overlap based on the dose responses at different positions in the ellipses, with the overlap for MCF-10A cells being most pronounced. There is a clear distinction between the entrance plateau region and the position in the distal fall of region of the SOBP for the MCF-10A cells; this clearly indicates an increase variation in the cancerous cell's response to proton irradiation at different regions of the beam. When comparing the 95% confidence ellipses for the Dmax 40% of both cells, there is clear difference in the dose response relationship (Figure 7) between the two cell lines. This agrees with the observations obtained with the reference radiation, were isolated ellipses were also observed (Figure 7). The confidence ellipses for MCF-7 cells are relatively larger for all positions especially at the distal 40% region (Figure 7), further signifying an increased variation in radiosensitivity for cells irradiated with protons.

Bromodeoxyuridine (BrdU) and flow cytometric results

Flow cytometry evaluated the fraction of BrdU incorporation in MCF-7 and MCF-10A cells, which is an indication of the percentage of cells in S-phase. This analysis revealed that MCF-7 cells spend a longer time in the S-phase compared to the MCF-10A cells. As reflected by the flow cytometric analysis, 53% of MCF-7 cells were in S-phase, whereas, 43% of MCF10 was noted for the same phase.

Variation in relative biological effectiveness (RBE)

To calculate the RBE_{ep}, the iso-effective doses were calculated for different levels of biological effects. Using the linear-quadratic model and the α- and β-values listed in Table 1, the iso-effective doses were calculated at biological effects ranging between 100 up to 500 MNi/1000 BNCs. Table 2 demonstrate the iso-effective doses calculated for MCF10-A and MCF-7 cells respectively.

For the non-cancerous breast cells, the dose decreased with depth between 1.44 Gy and 0.96 Gy for 200 MNi/1000 BNCs and from 2.82 Gy to 2.06 Gy for 400 MNi/1000 BNCs as indicated in Table 2. For MCF-7 cells the proton dose decreases from 2.26 Gy in the entrance plateau to 1.48 Gy at 40% Dmax, at a level of 200 MNi/1000 BNCs. For an effect of 400 MNi/1000 BNCs the dose decreased from 4.90 Gy to 2.88 Gy for the cancerous breast cell lines. The resulting RBE_{ep} values are plotted in Figure 8A. As expected, the RBE_{ep} decreases with dose, from a minimum of 1.05 to a maximum of 1.43 for an iso-effect of 300 MNi/1000 BNCs for MCF-10A cells. The RBE_{ep} calculated for the MCF-7 cell line can be seen in Figure 8B. However, in this case, the RBE_{ep} slightly increased with radiation dose. For the cancerous cells, there was also an increase in RBE_{ep} from 1.17 to 1.61 for an iso-effect of 300 MNi/1000 BNCs. It was anticipated that the RBE_{ep} would increase with depth throughout the proton beam for both the cancerous and normal breast cell lines. However, for the cancerous MCF-7 cells, the RBE_{ep} was higher at the 80% Dmax compared to the 40% Dmax which is located further down in the distal region of the proton beam.

Discussion

Conventionally, the ability to deliver large doses of radiation to a tumor has been limited by radiation-induced toxicity to normal

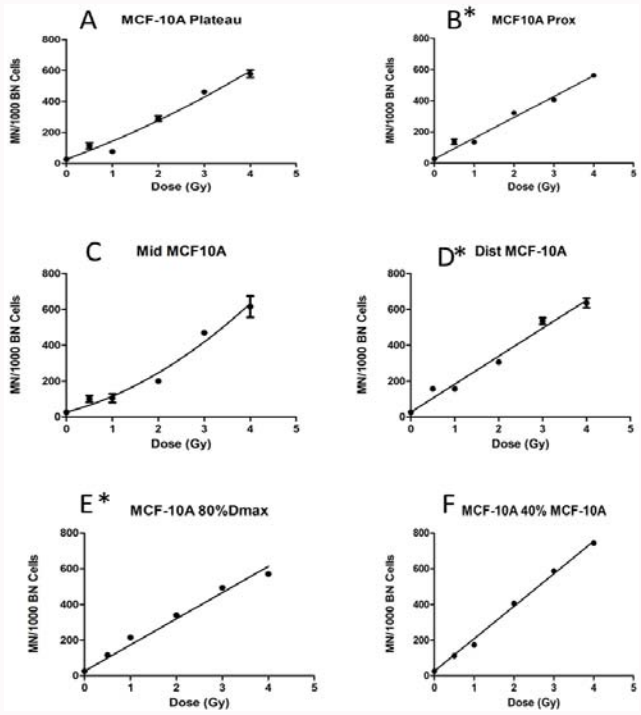

Figure 2: Best fit data graphs calculated from the MN formations per 1000 BN cells for the MCF-10A cells along the SOBP, from (A) the entrance plateau region to (F) the distal 40% region. (* graphs that were re-fitted and the process repeated until all the highest-order interactions were still significant at the 5% level).

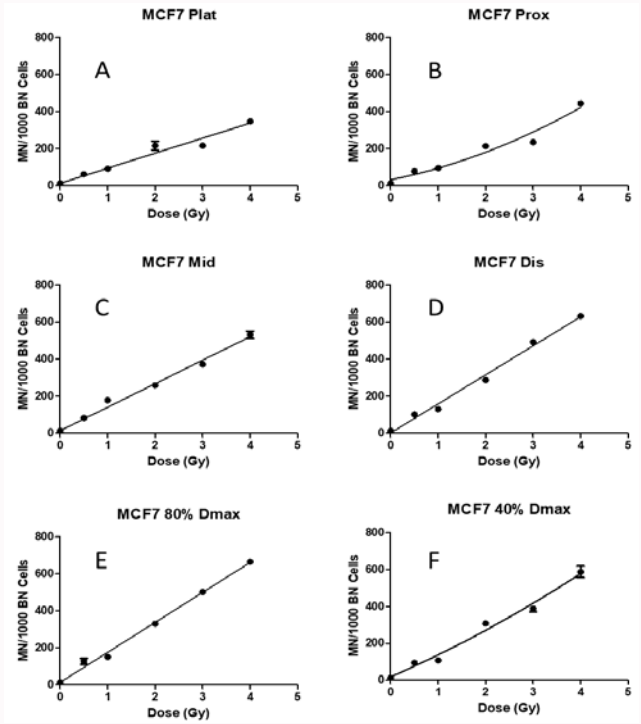

Figure 3: Best fit data graphs calculated from the MN formations per 1000 BN cells for the MCF-7 cells at different positions along the SOBP, beam from (A) the entrance plateau region to (F) the distal 40% region.

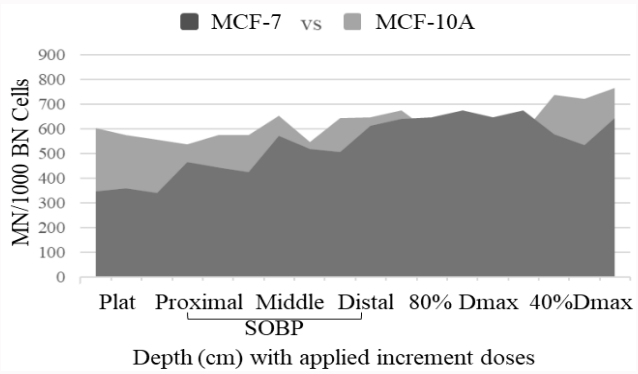

Figure 4: Area graph showing the MN formations per 1000 BN cells for both MCF-7 and MCF-10A cells for the highest dose in the proton beam depth.

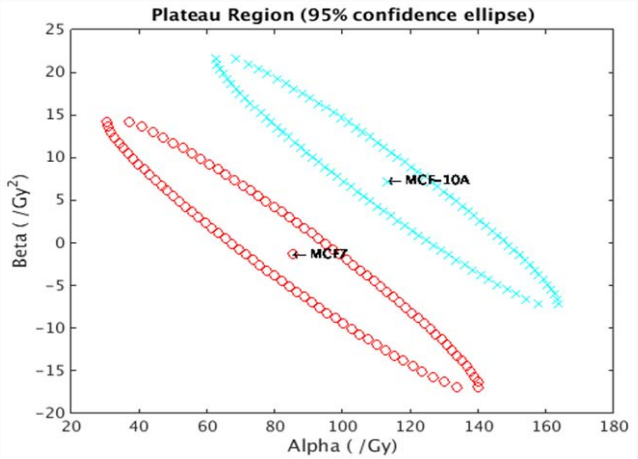

Figure 5: 95% confidence ellipses for both cell lines in the plateau region. MCF-10A cells (turquoise) with a higher α/β ratio compared to the MCF-7 cells (red).

surrounding tissues. The main objective of this study was to understand the biological effect and response of protons on two different human breast cell lines. Despite the growing interest and experience in the clinical use of PT, the radiobiological differences after proton compared to photon irradiation remains to be completely elucidated [36]. PT currently uses a generic RBE of 1.1, nearly equivalent to the RBE of high-energy X-rays. However, there is growing experimental evidence data suggesting that the RBE of protons is significantly higher in the distal area of the Spread-Out Bragg Peak (SOBP) [37]. The debate is still ongoing and limits to reach the full potential of PT, as uncertainties in the RBE directly results in an uncertainty in the biological effective dose delivered to the patient. This leads to a potential extension of the bio-effective range, which could contribute to normal tissue complications. Most published data focus on cell killing using colony survival assays with tumor cells, which is not the most representative assay to predict side effects observed in normal tissue [38-40].

Based on reported literature on the study of breast cells, the shape of the cell is assumed to be spherical with appropriate modifications in geometry and boundary conditions [41]. Two types of breast cells, namely MCF-10A and MCF-7 were thus considered for the current study with comparable doubling time reported [42]. Consequently, the approach was to use cancerous and non-cancerous epithelial cells that are similar in structure, location, and their functionality. It is well known that different breast cell lines respond differently to the same type of radiation treatment [43]. However, cells of different origin, such as endothelial cells, should further be considered as a potentially

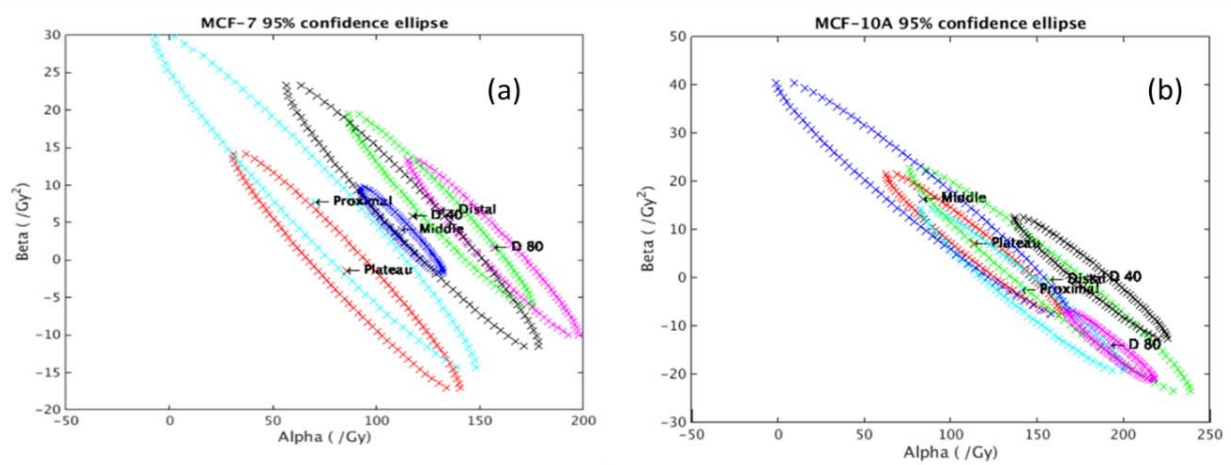

Figure 6: 95% Confidence ellipses for the (a) MCF-7 and (b) MCF-10A cells for different regions in the proton beam.

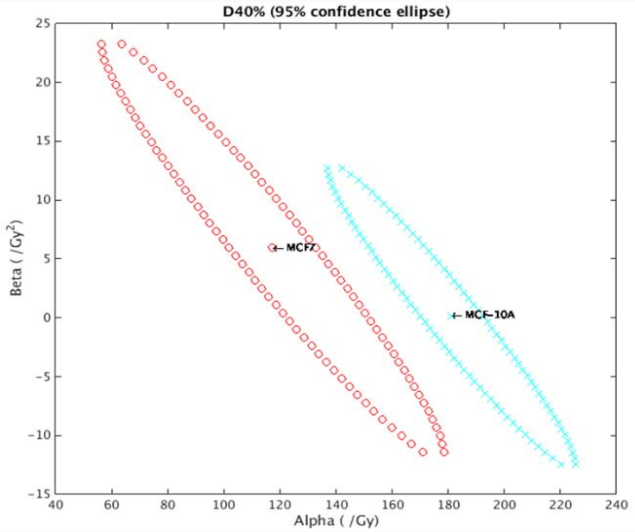

Figure 7: The 95% Confidence ellipses at the distal 40% for both cell lines. The 95% Confidence ellipse for the MCF-10 cell (turquoise) are shifted to the right of the graph indicating a higher α-value compared to the MCF-7 cells (red).

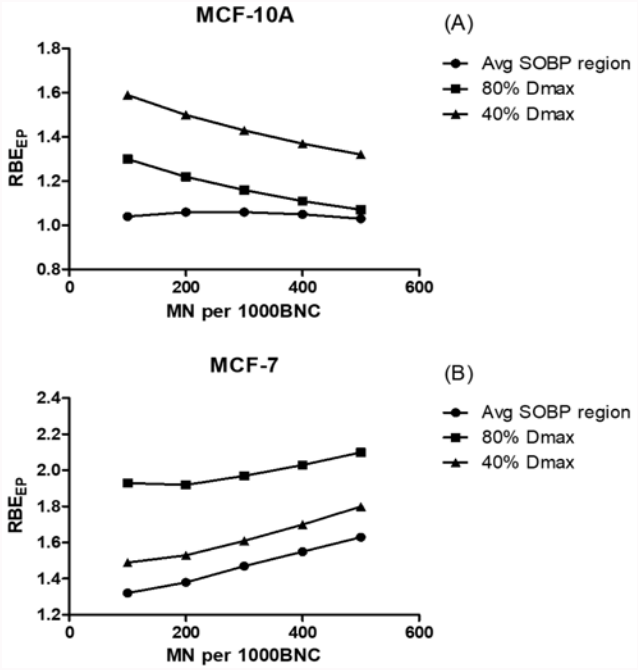

Figure 8: RBE$_{ep}$ calculated based on the plateau region as reference radiation for (A) MCF-10A, and (B) MCF-7 cells.

more relevant cell line to address concerns relating to late effects of proton irradiations. In a study where *γ*-rays radiation was used to investigate the radiosensitivity of these cell lines with both clonogenic cell survival and DNA DSB repair assays, it was clear that MCF-10A cells were more radiosensitive compared to the cancerous cell lines [44]. Choi et al. determined the RBE of 230 MeV protons mid-SOBP, compared to 6 MV X-rays, in ten human breast cell lines, including 5 Triple-Negative Breast Cancer (TNBC) cell lines. Clonogenic survival assays revealed a wide range of proton RBE across the breast cell lines, but the non-cancerous MCF-10A cell line appeared not as more radiosensitive than the MCF-7 cell line for a survival fraction from a clonogenic survival assay at 2 Gy [45]. When the effect of proton beams on DNA methylation were evaluated in the MCF-10A and MCF-7 the non-cancerous breast cell line, an increased hypermethylation was observed in the MCF-10A cells, suggesting that the non-cancerous cell was more resistant to the proton irradiation with respect to genomic instability [46]. Generally, the cancerous cells were more radio resistant compared to the normal breast cell lines in this study and concur with previous findings [43,47]. However, it is clear that the results of previously published studies and our own dataset contradict each other and it is therefore difficult to draw a final conclusion on the radiosensitivity of MCF-10A cells compared to MCF-7 cells for proton irradiation.

Although, the impact of the various DNA repair assays on the cytotoxicity and genotoxicity due to ionizing radiation are well documented, with additional information on senescence, cell cycle, DNA DSB or cell survival, the preliminary assessment using the CBMN assay to quantify cytogenetic damage were preferred [48]. The CBMN assays were also previously used to explore radiosensitivity in Chinese hamster cells for two low-energy proton beam (0.88 and 5.04 MeV) [49]. However, it is important to take into consideration that these shallow low-energy proton beams are known to have a higher LET values than the high-energy proton beams used in clinical practice. The lowest dose used in that study was 0.5 Gy and MNi per

1000 BN cells did increase when compared to the controlled groups for both cells, indicating a significant increase in DNA damage which was in agreement previously published work [50].

The increase in biological damage per unit dose at the different depths is reflected in the RBE variation along the SOBP. In this study, the variation in RBE_{ep} was between 0.99 to 1.99 and 0.92 to 1.6 for the cancerous cells and the normal breast cell, respectively. As expected, the RBE_{ep} was higher for the MCF-7 cell line that accumulates and repairs a large amount of sub-lethal damage and is more radio resistant. Previous studies measured with the colony survival assay as biological end point reported RBE increases in the middle of the SOBP to 1.2 and also from 1.1 to 1.2 at the middle of the SOBP when the SOBP was increased to 7 cm [51,52]. The distal edge region showed an increase in radiosensitivity for both cells which was in line with studies done for various cell lines using a 2 Gy fractionation dose, where RBE_{ep} increases up to 1.35 on average at the distal fall-off were reported [28]. However, the distal 40% Dmax position for the non-cancerous cell line did not coincide with previous studies, where a continuous increase in RBE_{ep} in the far distal edge of the proton beam was reported [28]. This can possibly be explained by a variation in proton beam energy during the experiment, resulting in a range uncertainty and output corrections were applied as described by Zhao et al. [53]. These range uncertainties effects on biological models were previously explored by Paganetti et al. [54].

The ratio of the dose values needed to reach the same level of biological effect when comparing two radiation modalities should be carefully considered while planning a radiotherapy treatment with charged particles. In the case of proton therapy, the effectiveness of the radiation damaging process is due to changes in the microscopic pattern of energy deposition of a charged particle shortly before its stops usually located near a critical structure or cells that lines the surfaces of organs including skin, blood vessels, urinary tract, etc. A recent study was developed for assessing the LET and RBE in proton therapy beams using couples of differently doped thermoluminescent detectors showed comparable results with Monte Carlo computer simulations [55]. The results of a clonogenic cell survival assay study performed using Chinese Hamster Ovary (CHO) cells exposed in the same detector positions revealed a corresponding trend for assessing the LET and RBE in proton therapy. Similarly, with comparable positions, a study by Cunningham et al. [56], exposed the LET values of 0.90, 3.81 and 7.17 keV/μm representing the radiation quality at the entrance, the end of the proton track and the 80% distal fall-off respectively, revealing a direct consequence of the increase in ionization density with depth along the SOBP, which is also reflected in the increasing LET values particularly at the distal fall-off.

BrdU (an analogy of the DNA precursor thymidine) is incorporated into newly synthesized DNA by cells entering and progressing through the S-phase (DNA synthesis) of the cell cycle. The levels of cell-associated BrdU, stained with a dye that binds to DNA such as 7-Amino-Actinomycin D (7-AAD), are then measured by flow cytometry. With this combination, two-color flow cytometric analysis permits the enumeration and characterisation of cells that are actively synthesizing DNA (BrdU incorporation) in terms of their cell cycle position. Each cycle phase was measured as a percentage in terms of the time it spends in each checkpoint. Cells that divide frequently are more radiation-sensitive than those that divide rarely thus, tissues that consist of rapidly dividing cells are similarly radiation-sensitive [57,58]. MCF-7 cells spend approximately 10% more time in the S-phase when compared to MCF-10A; this could possibly explain the increase in resistance of the MCF-7 cells. Nevertheless, DNA synthesis for cancer cell lines are extended as doubling time for MCF-7 cells is 26 h to 34 h, while MCF-10A has a doubling time of 10 h to 21 h [42,51,59-61]. MCF-10A cells are known to grow faster than MCF-7, therefore the result that MCF-7 cells are more resistant than MCF-10A is intriguing. Based on the BrdU assay and flow cytometry results, a possible explanation could be the variation during the doubling time in each culture. A comparison of these two cell lines can only be confirmed on the BrdU results which found that the MCF-10 cell line was in a more sensitive phase of the cell cycle than the MCF-7 cell line at the time of irradiation. The slightly higher S-phase fraction of MCF-7 cells, known to be the most radio resistant phase of the cell cycle, might explain the difference in radiosensitivity with the MCF-10A cells [62]. However, since these results were unrepeated and lack any range of deviation, it is a bit controversial to make such a claim with only a 10% difference.

The clinical importance of this study should be understood in terms of the α/β ratios for protons for both cell lines. The ellipse represents the inherent radiosensitivity of the cell lines (α-value) as well as the capacity to accumulate repairable damage (β-value). The confidence ellipses around the mean α- and β-value estimated were segregated for both cell lines. The zero β-value for MCF-7 cells may well be the result of the 3 Gy dose points that was somehow underestimated in the experimental work Figure 3A. It was unfortunately not possible to repeat the proton irradiations to confirm the findings, due to beam time restrictions. Therefore, the β-value for the MCF-10A cell line was used to fit the data for the MCF-7 cells to calculate the α/β ratios. The α/β ratio for MCF-7 cells was then calculated to be 8 Gy to compare to 16 Gy for MCF10A cells.

The α/β ratio is a measure of the importance of fractionation in determining the biological effective dose [63,64]. For fractionated PT the MCF10A cells will repair less damage between fractions compared to the MCF-7 cells, which negates the advantage of fractionation [65]. Based on the results of this study, a hypo-fractionated stereotactic treatment protocol might be more beneficial for breast cancer patients [66]. Although, previous hypo-fractionation studies demonstrated comparable results in late toxicities and concluded to be non-inferior to conventional fractionation with varying biological effective doses, the tumors response due to its microenvironment to radiation treatment remains unexplored [67,68].

The above argument is based only on the radiosensitivity of the two cells when exposed in the entrance plateau region. Further analysis of the 95% confidence ellipse of both cell lines showed a clear increase of the α-value toward the distal portion of the beam and indicated an increase in LET and ionization density in this region, resulting in more complex DNA damage [69]. Considering that the α and β parameters gradually increase with depth for protons for both cells, of clinical importance is a non-homogeneous dose within the targeted area and the unwanted high dose behind the targeted area as emphasized in former studies especially for pediatric tumors, and more recently for breast cancer patients [26,70,71]. Therefore, distal energy modulation could be investigated especially with larger tumors [72]. It is clear that the modulation of the SOBP should be such that less radiation is applied to the distal part to keep the biological effectiveness analogous [73]. A persisted observation in view of the 95% confidence ellipses for the non-cancerous breast cell lines are more compressed compared to the cancerous cell lines indicating an

increase in variance of radiosensitivity in the cancerous cells, based on the α-value, to proton radiation.

Since the RBE increased for lower doses and the rationality of the linear quadratic model in the lower dose region has been questioned during this study, it would be beneficial to incorporate even lower dose points in future studies. Although this study indicated a clear variation in radiosensitivity for the two breast cell lines, future investigations should consider more radiobiological endpoints where DNA-damage repair can be assessed by focusing on repair-related proteins [74].

Conclusion

Breast cancer is the most commonly diagnosed cancer among woman in South Africa, with almost half a million woman dying of this disease [75,76]. Therefore, a resilient purpose should be focused on treatment efforts, including PT. However, the concern around the uncertainties in RBE and LET at the distal region of the beam, close to critical structures, remains a major concern [77]. The increased survival of the cancerous breast cells compared to normal breast cells, might call for the consideration of hypofractionated PT. While more biological endpoints should be investigated, and *in vivo* models should be used to improve our understanding of proton radiobiology, this study adds significant information to the existing evidence base that there is an increase in RBE in the distal fall-off region relative to the proton beam entrance plateau however, cells of different origin should further be considered to address concerns relating to late effects of proton irradiations. Disregarding RBE variations could lead to suboptimal proton plans, resulting in lower doses to the tumor and hot spots in organs at risk. Future studies therefore could include cell lines of different origins to therefore, these results could be used by the modeling community to further develop biologically motivated treatment planning for proton therapy.

Author Contributions

PP, XM, ES and CV conceptualized and designed the experiments. PP, XM, SN, and CV performed the irradiation experiments, dosimetry, and laboratory work. PP and ES analyzed the data and PP performed the statistical analysis. PP, ES, XM, SN, JS and CV wrote the paper. All authors contributed to and approved the final version of the article.

Funding

This research was funded by NRF (National Research Foundation) under the Southern African Institute for Nuclear Technology and Sciences (SAINTS) scholarship.

References

1. Murugan N, Chb MB, Sa FCS, Dickens C, Pisa P, Mccormack V, et al. Down-staging of breast cancer in the pre-screening era: Experiences from Chris Hani Baragwanath Academic Hospital, Soweto, South Africa. S Afr Med J. 2014;104(5):2012-5.
2. Hamdi Y, Abdeljaoued-Tej I, Zatchi AA, Abdelhak S, Boubaker S, Brown JS, et al. Cancer in Africa: The untold story. Front Oncol. 2021;11:650117.
3. Lambert M, Mendenhall E, Kim AW, Cubasch H, Joffe M, Norris SA. Health system experiences of breast cancer survivors in urban South Africa. Womens Health (Lond). 2020;16:1745506520949419.
4. Barnett GC, West CML, Dunning AM, Elliott RM, Coles CE, Pharoah PDP, et al. Normal tissue reactions to radiotherapy: Towards tailoring treatment dose by genotype. Nat Rev Cancer. 2009;9(2):134-42.
5. Taylor CW, Kirby AM. Cardiac side-effects from breast cancer radiotherapy. Clin Oncol. 2015;27(11):621-9.
6. Hill-Kayser CE, Both S, Tochner Z. Proton therapy: Ever shifting sands and the opportunities and obligations within. Front Oncol. 2011;1:24.
7. Musielak M, Suchorska WM, Fundowicz M, Milecki P, Malicki J. Future perspectives of proton therapy in minimizing the toxicity of breast cancer radiotherapy. J Pers Med. 2021;11(5):410.
8. Jermann M. Particle therapy patient statistics (per end of 2016) (Data collected by the Particle Therapy Co-Operative Group). PTCOG. 2017;2016-7.
9. Levin WP, Kooy H, Loeffler JS, DeLaney TF. Proton beam therapy. Br J Cancer. 2005;93(8):849-54.
10. Hashemi Z, Tatari M, Naik H. Simulation of dose distribution and secondary particle production in proton therapy of brain tumor. Reports Pract Oncol Radiother. 2020;25(6):927-33.
11. Hug EB, Slater JD. Proton radiation therapy for pediatric malignancies: status report. Strahlenther Onkol. 1999;175 Suppl 2:89-91.
12. Cuaron JJ, MacDonald SM, Cahlon O. Novel applications of proton therapy in breast carcinoma. Chin Clin Oncol. 2016;5(4):52.
13. Clarke M, Collins R, Darby S, Davies C, Elphinstone P, Evans V, et al. Effects of radiotherapy and of differences in the extent of surgery for early breast cancer on local recurrence and 15-year survival: An overview of the randomised trials. Lancet. 2005;366(9503):2087-106.
14. Hooning MJ, Aleman BMP, Van Rosmalen AJM, Kuenen MA, Klijn JGM, Van Leeuwen FE. Cause-specific mortality in long-term survivors of breast cancer: A 25-year follow-up study. Int J Radiat Oncol Biol Phys. 2006;64(4):1081-91.
15. Darby SC, Ewertz M, McGale P, Bennet AM, Blom-Goldman U, Brønnum D, et al. Risk of ischemic heart disease in women after radiotherapy for breast cancer. N Engl J Med. 2013;368(11):987-98.
16. Lomax AJ, Bohringer T, Bolsi A, Coray D, Emert F, Goitein G, et al. Treatment planning and verification of proton therapy using spot scanning: Initial experiences. Med Phys. 2004;31(11):3150-7.
17. MacDonald SM, Patel SA, Hickey S, Specht M, Isakoff SJ, Gadd M, et al. Proton therapy for breast cancer after mastectomy: Early outcomes of a prospective clinical trial. Int J Radiat Oncol Biol Phys. 2013;86(3):484-90.
18. Strom EA, Ovalle V. Initial clinical experience using protons for accelerated partial-breast irradiation: Longer-term results. Int J Radiat Oncol Biol Phys. 2014;90(3):506-8.
19. Kozak KR, Smith BL, Adams J, Kornmehl E, Katz A, Gadd M, et al. Accelerated partial-breast irradiation using proton beams: Initial clinical experience. Int J Radiat Oncol Biol Phys. 2006;66(3):691-8.
20. Wang W, Wainstein R, Freixa X, Dzavik V, Fyles A. Quantitative coronary angiography findings of patients who received previous breast radiotherapy. Radiother Oncol. 2011;100(2):184-8.
21. Ares C, Khan S, MacArtain AM, Heuberger J, Goitein G, Gruber G, et al. Postoperative proton radiotherapy for localized and locoregional breast cancer: Potential for clinically relevant improvements? Int J Radiat Oncol Biol Phys. 2010;76(3):685-97.
22. Xu N, Ho MW, Li Z, Morris CG, Mendenhall NP. Can proton therapy improve the therapeutic ratio in breast cancer patients at risk for nodal disease? Am J Clin Oncol. 2014;37(6):568-74.
23. Gulliford SL, Prise KM. Relative biological effect/linear energy transfer in proton beam therapy: A primer. Clin Oncol. 2019;31(12):809-12.
24. Murshed H. Chapter 1 - Radiation Physics, Dosimetry, and Treatment Planning. In: Murshed HBT-F of RO 3rd Ed. Medical Physics Publishing Madison, Wisconsin; 2019. p. 3-37.

25. Jones B, McMahon SJ, Prise KM. The radiobiology of proton therapy: Challenges and opportunities around relative biological effectiveness. Clin Oncol (R Coll Radiol). 2018;30(5):285-92.

26. Marteinsdottir M, Wang CC, McNamara AL, Depauw N, Shin J, Paganetti H. The impact of variable RBE in proton therapy for left-sided breast cancer when estimating normal tissue complications in the heart and lung. Phys Med Biol. 2020.

27. Mohan R, Peeler CR, Guan F, Bronk L, Cao W, Grosshans DR. Radiobiological issues in proton therapy. Acta Oncol. 2017;56(11):1367-73.

28. Paganetti H. Relative Biological Effectiveness (RBE) values for proton beam therapy. Variations as a function of biological endpoint, dose, and linear energy transfer. Phys Med Biol. 2014;59(22):419-72.

29. Guogytė K, Plieskienė A, Ladygienė R, Vaisiūnas Ž, Sevriukova O, Janušonis V, et al. Assessment of correlation between chromosomal radiosensitivity of peripheral blood lymphocytes after *in vitro* irradiation and normal tissue side effects for cancer patients undergoing radiotherapy. Genome Integr. 2017;8:1.

30. Vandersickel V, Mancini M, Slabbert J, Marras E, Thierens H, Perletti G, et al. The radiosensitizing effect of Ku70/80 knockdown in MCF10A cells irradiated with X-rays and p(66)+Be(40) neutrons. Radiat Oncol. 2010;5:30.

31. Mosconi M, Musonza E, Buffler A, Nolte R, Röttger S, Smit FD. Characterisation of the high-energy neutron beam at iThemba LABS. Radiat Meas. 2010;45(10):1342-5.

32. Theron T, Slabbert J, Serafin A, Böhm L. The merits of cell kinetic parameters for the assessment of intrinsic cellular radiosensitivity to photon and high linear energy transfer neutron irradiation. Int J Radiat Oncol Biol Phys. 1997;37(2):423-8.

33. Slabbert JP, Binns PJ, Jones HL, Hough JH. A quality assessment of the effects of a hydrogenous filter on a p(66)Be(40) neutron beam. Br J Radiol. 1989;62(743):989-94.

34. Lopez J, Robles I, Martinez-Planell R. Students' understanding of quadratic equations. Int J Mathemat Edu Science Tech. 2016;47(4):552-72.

35. Slabbert J, Martinez J, De Coster B-M, Gueulette J. Increased proton relative biological effectiveness at the very end of a spread-out Bragg peak for jejunum irradiated *ex vivo*. Int J Part Ther. 2015;2(1):37-43.

36. Vanderwaeren L, Dok R, Verstrepen K, Nuyts S. Clinical progress in proton radiotherapy: Biological unknowns. Cancers. 2021;13(4):604.

37. Ilicic K, Combs SE, Schmid TE. New insights in the relative radiobiological effectiveness of proton irradiation. Radiat Oncol. 2018;13(1):6.

38. Radulovic V, Heider T, Richter S, Moertl S, Atkinson MJ, Anastasov N. Differential response of normal and transformed mammary epithelial cells to combined treatment of anti-miR-21 and radiation. Int J Radiat Biol. 2017;93(4):361-72.

39. Mubeen AA, Chaudhary S, Arun Barathwaj R, Chandrashekara CV. Dynamic analysis of MCF-10A and MCF-7: A simulation approach. Vibroengineering Procedia. 2020;30:126-32.

40. Larsson P, Engqvist H, Biermann J, Rönnerman EW, Forssell-Aronsson E, Kovács A, et al. Optimization of cell viability assays to improve replicability and reproducibility of cancer drug sensitivity screens. Sci Rep. 2020;10(1):5798.

41. Niazvand F, Orazizadeh M, Khorsandi L, Abbaspour M, Mansouri E, Khodadadi A. Effects of quercetin-loaded nanoparticles on MCF-7 human breast cancer cells. Medicina (Kaunas). 2019;55(4):114.

42. Afshar AS, Nematpour FS, Meshkani M, Khafi A. Growth inhibition of human breast cancer cells and down-regulation of ODC1 and ADA genes by nepeta binaloudensis. Rev Bras Farmacogn. 2017;27(1):84-90.

43. Masoudi-Khoram N, Abdolmaleki P, Hosseinkhan N, Nikoofar A, Mowla SJ, Monfared H, et al. Differential miRNAs expression pattern of irradiated breast cancer cell lines is correlated with radiation sensitivity. Sci Rep. 2020;10(1):9054.

44. Villalobos M, Becerra D, Nunez MI, Valenzuela MT, Siles E, Olea N, et al. Radiosensitivity of human breast cancer cell lines of different hormonal responsiveness. Modulatory effects of oestradiol. Int J Radiat Biol. 1996;70(2):161-9.

45. Choi C, Park S, Cho WK, Choi DH. Cyclin D1 is associated with radiosensitivity of triple-negative breast cancer cells to proton beam irradiation. Int J Mol Sci. 2019;20(19):4943.

46. Kim B, Bae H, Lee H, Lee S, Park JC, Kim KR, et al. Proton beams inhibit proliferation of breast cancer cells by altering DNA methylation status. J Cancer. 2016;10;7(3):344-52.

47. Gray M, Turnbull AK, Ward C, Meehan J, Martínez-Pérez C, Bonello M, et al. Development and characterisation of acquired radioresistant breast cancer cell lines. Radiat Oncol. 2019;14(1):64.

48. Paget V, Kacem MB, Santos MD, Benadjaoud MA, Soysouvanh F, Buard V, et al. Multiparametric radiobiological assays show that variation of X-ray energy strongly impacts relative biological effectiveness: comparison between 220 kV and 4 MV. Sci Rep. 2019;9(1):14328.

49. Sgura A, Antoccia A, Cherubini R, Dalla Vecchia M, Tiveron P, Degrassi F, et al. Micronuclei, CREST-positive micronuclei and cell inactivation induced in Chinese hamster cells by radiation with different quality. Int J Radiat Biol. 2000;76(3):367-74.

50. Vral A, Fenech M, Thierens H. The micronucleus assay as a biological dosimeter of *in vivo* ionising radiation exposure. Mutagenesis. 2011;26(1):11-7.

51. Gueulette J, Bohm L, De Coster BM, Vynckier S, Octave-Prignot M, Schreuder AN, et al. RBE variation as a function of depth in the 200-MeV proton beam produced at the National Accelerator Centre in Faure (South Africa). Radiother Oncol. 1997;42(3):303-9.

52. Paganetti H. Significance and implementation of RBE variations in proton beam therapy. Technol Cancer Res Treat. 2003;2(5):413-26.

53. Zhao Q, Wu H, Cheng CW, Das IJ. Dose monitoring and output correction for the effects of scanning field changes with uniform scanning proton beam. Med Phys. 2011;38(8):4655-61.

54. Carabe A, Moteabbed M, Depauw N, Schuemann J, Paganetti H. Range uncertainty in proton therapy due to variable biological effectiveness. Phys Med Biol. 2012;57(5):1159-72.

55. Parisi A, Chiriotti S, Saint-Hubert MD, Hoey OV, Vandevoorde C, Beukes P, et al. A novel methodology to assess linear energy transfer and relative biological effectiveness in proton therapy using pairs of differently doped thermoluminescent detectors. Phys Med Biol. 2019;64(8):085005.

56. Cunningham C, de Kock M, Engelbrecht M, Miles X, Slabbert J, Vandevoorde C. Radiosensitization effect of gold nanoparticles in proton therapy. Front Public Health. 2021;9:699822.

57. Hafer K, Rivina L, Schiestl RH. Cell cycle dependence of ionizing radiation-induced DNA deletions and antioxidant radioprotection in *Saccharomyces cerevisiae*. Radiat Res. 2010;173(6):802-8.

58. Yashar CM. Chapter 23 - Basic Principles in Gynecologic Radiotherapy. Philip JS, editor. In: Creasman WTBT-CGO. 8th Ed. Philadelphia: Mosby; 2012. p. 659-680.e3.

59. Coller HA. What's taking so long? S-phase entry from quiescence versus proliferation. Nat Rev Mol Cell Biol. 2007;8(8):667-70.

60. Cecchini MJ, Amiri M, Dick FA. Analysis of cell cycle position in mammalian cells. J Vis Exp. 2012;21;(59):3491.

61. Corbin EA, Adeniba OO, Cangellaris OV, King WP, Bashir R. Evidence of differential mass change rates between human breast cancer cell lines in culture. Biomed Microdevices. 2017;19(1):10.

62. Pajonk F, Vlashi E, McBride WH. Radiation resistance of cancer stem cells: The 4 R's of radiobiology revisited. Stem Cells. 2010;28(4):639-48.

63. Ray KJ, Sibson NR, Kiltie AE. Treatment of breast and prostate cancer by hypofractionated radiotherapy: Potential risks and benefits. Clin Oncol (Royal Coll Radiol). 2015;27(7):420-6.

64. Hawkins RB. Effect of heterogeneous radio sensitivity on the survival, alpha beta ratio and biologic effective dose calculation of irradiated mammalian cell populations. Clin Transl Radiat Oncol. 2017;4:32-8.

65. van Leeuwen CM, Oei AL, Crezee J, Bel A, Franken NAP, Stalpers LJA, et al. The Alfa and beta of tumours: A review of parameters of the linear-quadratic model, derived from clinical radiotherapy studies. Radiat Oncol. 2018;13(1):96.

66. Laine AM, Pompos A, Timmerman R, Jiang S, Story MD, Pistenmaa D, et al. The role of hypofractionated radiation therapy with photons, protons, and heavy ions for treating extracranial lesions. Front Oncol. 2015;5:302.

67. Wang SL, Fang H, Song YW, Wang WH, Hu C, Liu YP, et al. Hypofractionated versus conventional fractionated postmastectomy radiotherapy for patients with high-risk breast cancer: A randomised, non-inferiority, open-label, phase 3 trial. Lancet Oncol. 2019;20(3):352-60.

68. Hill RP. The changing paradigm of tumour response to irradiation. Br J Radiol. 2017;90(1069):20160474.

69. Carter RJ, Nickson CM, Thompson JM, Kacperek A, Hill MA, Parsons JL. Complex DNA damage induced by high linear energy transfer alpha-particles and protons triggers a specific cellular DNA damage response. Int J Radiat Oncol Biol Phys. 2018;100(3):776-84.

70. Jin H, Hsi W, Yeung D, Li Z, Mendenhall NP, Marcus RB. Dosimetric characterization of whole brain radiotherapy of pediatric patients using modulated proton beams. J Appl Clin Med Phys. 2011;12(2):3308.

71. Wang CC, McNamara AL, Shin J, Schuemann J, Grassberger C, Taghian AG, et al. End-of-range radiobiological effect on rib fractures in patients receiving proton therapy for breast cancer. Int J Radiat Oncol Biol Phys. 2020;107(3):449-54.

72. Buchsbaum JC, McDonald MW, Johnstone PAS, Hoene T, Mendonca M, Cheng CW, et al. Range modulation in proton therapy planning: A simple method for mitigating effects of increased relative biological effectiveness at the end-of-range of clinical proton beams. Radiat Oncol. 2014;9:2.

73. Flejmer AM, Nyström PW, Dohlmar F, Josefsson D, Dasu A. Potential benefit of scanned proton beam versus photons as adjuvant radiation therapy in breast cancer. Int J Part Ther. 2015;1(4):845-55.

74. Redon CE, Dickey JS, Bonner WM, Sedelnikova OA. Gamma-H2AX as a biomarker of DNA damage induced by ionizing radiation in human peripheral blood lymphocytes and artificial skin. Adv Space Res. 2009;43(8):1171-8.

75. Cancer Research UK. World cancer fact sheet, 2008. Int Agency Res Cancer. 2012;2008(2008):1-4.

76. Herbst MC. Cancer Association of South Africa (CANSA) fact sheet on the top ten cancers per population group top ten most common cancers of women top ten most common cancers of Asian men. CANSA. 2015;1-6.

77. Tommasino F, Durante M. Proton radiobiology. Cancers (Basel). 2015;7(1):353-81.